ENGINEERING TRANSACTIONS • *Engng. Trans.* • **65**, 2, 221–249, 2017
Polish Academy of Sciences • Institute of Fundamental Technological Research (IPPT PAN)
National Engineering School of Metz (ENIM) • Poznan University of Technology

Research Paper

Transfer Effects on an Unsteady MHD Mixed Convective Flow Past a Vertical Plate with Chemical Reaction

R. Srinivasa RAJU

Department of Mathematics
GITAM University, Hyderabad Campus
Rudraram, 502329, Telangana State, India
e-mail: srivass999@gmail.com

An attempt is made to study the effects of chemical reaction and combined buoyancy effects on an unsteady MHD mixed convective flow along an infinite vertical porous plate in the presence of hall current. A uniform magnetic field is applied in a direction normal to the porous plate. The governing coupled non-linear partial differential equations are solved using an efficient Galerkin finite element method. With the help of graphs, the effects of the various important parameters entering into the problem on the velocity, temperature, and concentration fields within the boundary layer are discussed. Also the effects of the pertinent parameters on the skin-friction coefficient and rates of heat and mass transfer in terms of the Nusselt number and Sherwood number are presented numerically in a tabular form. The results obtained show that the velocity, temperature, and concentration fields are appreciably influenced by the presence of chemical reaction, hall current, heat, and mass transfer. It is observed that the effect of Schmidt number and chemical reaction parameter is to decrease the velocity and concentration profiles in the boundary layer while the velocity profiles are increasing with increasing of hall parameter, Grashof numbers for heat and mass transfer. There is also considerable effect of hall current and chemical reaction on skin-friction coefficient and Nusselt number. In the present analysis various comparisons with previously published work are performed and the results are found to be in a good agreement.

Key words: heat and mass transfer, chemical reaction, MHD, hall current, Galerkin finite element method.

Notations

List of variables

$\overline{B}$ – magnetic induction vector,
B_o – intensity of the applied magnetic field [$\mathrm{A \cdot m^{-1}}$],
C – dimensionless species concentration of the fluid,
C_p – specific heat at constant pressure [$\mathrm{J \cdot kg^{-1} \cdot K}$],
C_∞ – concentration in the fluid far away from the plate [$\mathrm{kg \cdot m^{-3}}$],
C^* – species concentration of the fluid at the plate [$\mathrm{kg \cdot m^{-3}}$],
D – chemical molecular diffusivity [$\mathrm{m^2 \cdot s^{-1}}$],

D_T – coefficient of chemical thermal diffusivity, $M^1L^{-1}T^{-1}K^{-1}$,
$\overline{E}$ – electric field,
e – electron charge [C],
Gr – Grashof number for heat transfer,
Gr_c – Grashof number for mass transfer,
Pr – Prandtl number,
Sc – Schmidt number,
p_e – electron pressure $[\mathrm{N} \cdot \mathrm{m}^{-2}]$,
K_r – chemical reaction parameter,
T – temperature of the fluid [K],
T'_w – temperature of the plate [K],
T_∞ – fluid temperature far away from the plate [K],
t – time plate [s],
u – velocity component in x'-direction $[\mathrm{m} \cdot \mathrm{s}^{-1}]$,
$\overline{V}$ – velocity vector,
V_o – reference velocity $[\mathrm{m} \cdot \mathrm{s}^{-1}]$,
w – velocity component in z'-direction $[\mathrm{m} \cdot \mathrm{s}^{-1}]$,
g – acceleration due to gravity $[\mathrm{m} \cdot \mathrm{s}^{-2}]$,
$\overline{J}$ – electric current density vector,
K – permeability of the porous medium,
Ha – Hartmann number,
m – Hall parameter,
Nu – rate of heat transfer coefficient (or) Nusselt number,
Sh – rate of mass transfer coefficient (or) Sherwood number.

Greek symbols

β – coefficient of volume expansion $[\mathrm{K}^{-1}]$,
ρ – density of the fluid $[\mathrm{kg} \cdot \mathrm{m}^{-3}]$,
β^* – volumetric coefficient of expansion with concentration $[\mathrm{m}^3 \cdot \mathrm{kg}^{-1}]$,
υ – kinematic viscosity $[\mathrm{m}^2 \cdot \mathrm{s}^{-1}]$,
ω_e – electron frequency [Hz],
τ'_w – Shear stress $[\mathrm{N} \cdot \mathrm{m}^{-2}]$,
τ_1 – skin-friction due to velocity (u) $[\mathrm{N} \cdot \mathrm{m}^{-2}]$,
τ_2 – skin-friction due to velocity (w) $[\mathrm{N} \cdot \mathrm{m}^{-2}]$,
ωt – phase angle [rad],
Ω – angular frequency [Hz],
ω – frequency parameter,
θ – dimensionless temperature [K],
σ – electrical conductivity $[\Omega^{-1} \cdot \mathrm{m}^{-1}]$,
τ_e – electron collision time [s],
τ_i – ion collision time [s],
n_e – number of electron density,
ω_i – ion frequency [Hz],
κ – thermal conductivity $[\mathrm{W} \cdot \mathrm{m}^{-1} \cdot \mathrm{K}^{-1}]$.

Superscript
$'$ – dimensionless properties.
Subscripts
w – conditions on the wall,
∞ – free stream conditions.

1. Introduction

In recent years, the flow of fluids through porous media has been of principal interest because these are quite prevalent in nature. Such flows have attracted the attention of a number of scholars due to their application in many branches of science and technology: in the field of agriculture engineering they are used to study the underground water resources, seepage of water in riverbeds; in petroleum technology they help in studying the movement of natural gas, oil, and water through oil reservoirs; in chemical engineering their use is for filtration and purification processes. The convection problem in porous medium has also important applications in geothermal reservoirs and geothermal energy extractions. A comprehensive review of the studies of convective heat transfer mechanism through porous media has been made by Nield and Bejan [1]. Hiremath and Patil [2] studied the effect on free convection currents on the oscillatory flow through a porous medium, which is bounded by vertical plane surface of constant temperature. Fluctuating heat and mass transfer on three dimensional flow through a porous medium with variable permeability has been discussed by Sharma *et al.* [3]. Magnetohydrodynamics is currently undergoing a period of great enlargement and differentiation of subject matter. The interest in these new problems generates from their importance in liquid metals, electrolytes, and ionized gases. Unsteady hydromagnetic free convection flow of Newtonian fluid has been investigated by Helmy [4]. Chaudhary and Sharma [5] considered combined heat and mass transfer by laminar mixed convection flow from a vertical surface with induced magnetic field. Hydromagnetic unsteady mixed convection and mass transfer flow past a vertical porous plate immersed in a porous medium in presence of hall current was investigated by Sharma and Chaudhary [6]. El-Amin [7] considered the MHD free convection and mass transfer flow in a micropolar fluid over a stationary vertical plate with constant suction. Ramana Murthy *et al.* [8] discussed the effects of heat and mass transfer magnetohydrodynamic natural convective flow past an infinite vertical porous plate in presence of thermal radiation and hall current using Galerkin finite element method. The results of thermal radiation and heat absorption on an unsteady MHD free convective fluid flow over an infinite vertical plate embedded in porous medium in occurrence of thermal diffusion and diffusion thermo were discussed by Raju *et al.* [9]. Anand Rao and Srinivasa Raju [10] studied the effects of Hall currents, Soret, and Dufour on MHD flow and heat transfer along a porous flat plate with mass transfer. Sivaiah and Srinivasa Raju [11] studied the influence of Soret on an unsteady magnetohydrodynamics free convective flow past a semi-infinite vertical plate in the presence of viscous dissipation using Galerkin finite element method. Shiva Reddy Sheri and Srinivasa Raju [12] studied the effect of viscous dissipation on transient free convective flow past an infinite vertical porous plate in presence of magnetic field using Galerkin finite element method. Sivaiah Sheri and Srinivasa Raju [13] studied the effect of Hall current on heat and mass transfer viscous dissipative fluid flow with heat absorption using Galerkin finite element method. Rao *et al.* [14] found the numerical solutions by applying Galerkin finite element method on unsteady MHD heat and mass transfer flow past a semi-infinite moving vertical plate in presence of radiation and viscous dissipation. Anand Rao *et al.* [15] investigated the effect of hall current on MHD transient flow past an impulsively started infinite horizontal porous plate in a rotating fluid using Galerkin finite element method. The effects of heat and mass transfer on magnetohydrodynamic flow past a viscous fluid past a vertical plate under oscillatory suction velocity embedded in porous medium were studied by Anand Rao *et al.* [16].

Combined heat and mass transfer problems with chemical reaction are of importance in many processes and have, therefore, received a considerable amount of attention in recent years. In processes such as drying, evaporation at the surface of water body, energy transfer in wet cooling tower, and the flow in a desert cooler, heat and mass transfer occur simultaneously. Chemical reaction can be codified as either homogeneous or heterogeneous processes. A homogeneous reaction is one that occurs uniformly through a given phase. In contrast, a heterogeneous reaction takes place in a restricted region or within the boundary of a phase. A reaction is said to be first order, if the rate of reaction is directly proportional to the concentration itself which has many applications in different chemical engineering processes and other industrial applications such as polymer production, manufacturing of ceramics or glassware, and food processing [17]. Das *et al.* [18] considered the effects of first order chemical reaction on the flow past an impulsively started infinite vertical plate with constant heat flux and mass transfer. Muthucumarswamy and Ganesan [19] studied the effect of first order chemical reaction on flow past an impulsively started vertical plate in presence of uniform heat and mass flux. Muthucumarswamy [20] studied first order homogeneous chemical reaction on flow past infinite vertical plate. Das *et al.* [21] have studied the effect of mass transfer flow past an impulsively started infinite vertical plate with heat flux and chemical reaction. The chemical reaction effect on heat and mass transfer flow along a semi-infinite horizontal plate had been studied by Anjalidevi and Kandaswamy [22], and later it was extended for Hiemenz flow by Seddeek *et al.* [23], and for polar fluid by Patil and Kulkarni [24]. Salem and Abd El-Aziz [25] have reported the effect of hall currents and chemical reaction on hydromagnetic flow of a stretching vertical surface with internal heat generation or absorption. Ibrahim *et al.* [26] studied the effect of chemical reaction and radiation absorption on the unsteady MHD free convection flow past a semi-infinite vertical permeable moving plate with heat source and suction. A detailed numerical study was carried out for unsteady hydromagnetic natural convection heat and mass transfer with chemical reaction over a vertical plate in rotating system with periodic suction by Parida *et al.* [27]. Rajeswari *et al.* [28] have investigated chemical reaction, heat and mass transfer on nonlinear MHD boundary layer flow through a vertical porous surface in presence of suction. Mahdy [29] has studied the effect of chemical reaction and heat generation or absorption on double diffusive convection from vertical truncated cone in a porous media with variable viscosity. Recently, Muthucumaraswamy and Ravi Shankar [30] have discussed the combined effects of first order chemical reaction and thermal radiation on an unsteady flow past an accelerated isothermal infinite vertical plate. Jithender Reddy *et al.* [31] studied the effect of chemical reaction and radiation on unsteady magnetohydrodynamic free convection from an impulsively started infinite vertical plate with viscous dissipation. Sudhakar *et al.* [32] studied the effect of hall current on an unsteady MHD flow along a porous flat plate with thermal diffusion, diffusion thermo, and chemical reaction by using Galerkin finite element method. Sudhakar *et al.* [33] studied the effect of chemical reaction effect on an unsteady MHD free convection flow past an infinite vertical accelerated plate with constant heat flux, thermal diffusion and diffusion thermo by using Galerkin finite element method. Anand Rao *et al.* [34] studied the effect of chemical reaction on an unsteady MHD free convection fluid flow past a semi-infinite vertical plate embedded in a porous medium with heat absorption with the help of Galerkin finite element method. Srinivasa Raju [35] studied the combined effects of thermal-diffusion and diffusion-thermo on unsteady free convection fluid flow past an infinite vertical porous plate in presence of magnetic field and chemical reaction using finite element technique. Srinivasa Raju *et al.* [36] studied the application of finite element method to unsteady MHD free convection flow past a vertically inclined porous plate including thermal diffusion and diffusion thermo effects. Srinivasa Raju *et al.* [37] found both analytical and numerical results of unsteady magnetohydrodynamic free convective flow past an exponentially moving vertical plate with heat absorption and chemical reaction.

Taken the motivation given by their work, the objective of the present research was to study the effects of chemical reaction on an unsteady magnetohydrodynamic free convective flow past a vertical porous plate immersed in a porous medium in the presence of hall current. Hence, the purpose of this study was to extend Sharma and Chaudhary [6], to study the unsteady problem which includes internal chemical reaction for the first order. The governing equations were solved numerically using Galerkin finite element method. The present numerical results obtained under special cases are then compared with the analytical results of Sharma and Chaudhary [6] in absence of chemical reaction and found to agree very favourably. Dimensionless velocity, temperature, and concentration profiles are displayed graphically for different values of the parameters entering into the problem like Hartmann number, Prandtl number, Grashof number for heat transfer, Grashof number for mass transfer, Schmidt number, Hall parameter, Permeability parameter, and Chemical reaction parameter. The influence of these pertinent parameters on velocity, temperature, concentration fields are discussed through graphs and results are physically interpreted.

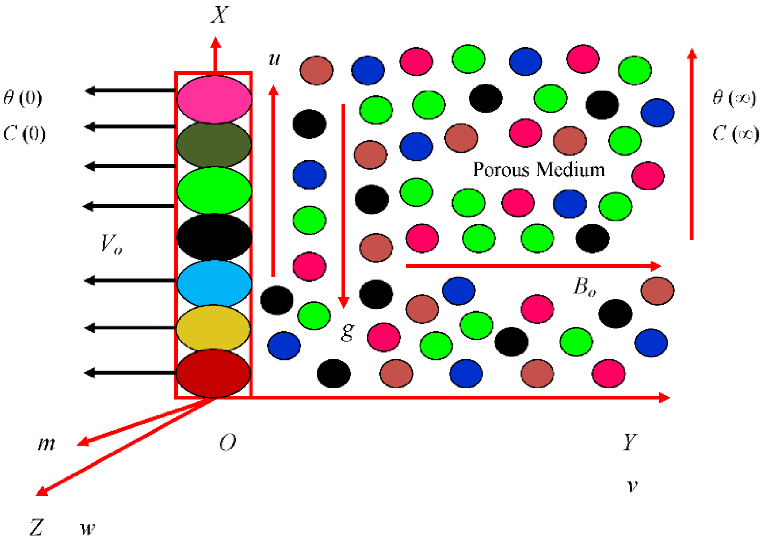

Fig. 1. Physical Model of the problem.

2. Mathematical formulation

The equations governing the motion of an incompressible viscous electrically conducting fluid in presence of a magnetic field are as follows:

- The continuity equation, defined by

$$\nabla \cdot \overline{v} = 0. \tag{2.1}$$

This is known as the incompressible continuity equation, because it is the form of the continuity equations obeyed by an incompressible fluid. Physically, incompressibility means that the density of an air parcel does not change. The momentum equation is based on the principle of conservation of momentum, i.e., that the time rate of change of momentum in a material region is equal to the sum of the forces on that region.

- The momentum equation is defined by

$$\rho\left[\frac{\partial\overline{v}}{\partial t}+(\overline{v}\cdot\nabla)\,\overline{v}\right]=-\nabla p+\overline{J}\times\overline{B}+\rho\overline{g}+\mu\nabla^2\overline{v}-\left[\frac{\mu}{k}\right]\overline{v}. \tag{2.2}$$

The first term on the left hand side is the local acceleration and the second term is known as the convective acceleration term. The second term is the term which makes the Navie-Stokes equation nonlinear, which is the source of the great complexity of the mathematics and physics of fluid motion. On the right hand side, the first term is the pressure gradient force, the third term represents the body force term, the fourth term is known as the viscous force, and the penultimate term in the square brackets denotes the bulk matrix resistance, i.e., Darcy term. The energy equation decouples from the rest of the Navier-Stokes equations for incompressible flow. This can be seen from a non-dimensionalisation of the energy equation by using the definition of the enthalpy.

- The energy equation is defined by

$$\rho Cp\left[\frac{\partial T}{\partial t}+(\overline{v}\cdot\nabla)\,T\right]=k\nabla^2T. \tag{2.3}$$

The first term on the left hand side is the temporal thermal gradient and the second term describes convection. On the right hand side, k is the thermal diffusivity and $\nabla^2 T$ is the thermal diffusion term. A continuity equation is an equation that describes the transport of some quantity. It is particularly simple and particularly powerful when applied to a conserved quantity, but it can be generalised to apply to any extensive quantity.

- The species continuity equation is defined by

$$\frac{\partial C}{\partial t}+(\overline{v}\cdot\nabla)\,C=D\nabla^2C+K_r'\,(C-C_\infty)\,, \tag{2.4}$$

where the opening term on the left hand side signifies the temporal concentration gradient and the second term describes the convection term. On the right hand side, the first term represents species diffusion and the last term is the chemical reaction term.

- The Kirchhoff's first law is given by

$$\nabla\cdot\overline{J}=0. \tag{2.5}$$

- The general Ohm's law, taking Hall effect into account is given by

$$\overline{J} + \frac{\omega_e \tau_e}{B_0}\left(\overline{J} \times \overline{B}\right) = \sigma\left(\overline{E} + \overline{v} \times \overline{B} + \frac{1}{e\eta_e}\nabla P_e\right), \tag{2.6}$$

- and Gauss's law of magnetism is given by

$$\overline{\nabla} \cdot \overline{B} = 0. \tag{2.7}$$

Consider an unsteady flow of an electrically conducting fluid past an infinite vertical porous flat plate coinciding with the x-axis, $y = 0$, taking into account the thermal diffusion, Hall current, and heat source in presence of a uniform transverse magnetic field. This investigation is restricted to the following assumptions:

i) All the fluid properties except the density in the buoyancy force term are constant.
ii) The plate is electrically non-conducting.
iii) The magnetic Reynolds number is so small that the induced magnetic field may be neglected.
iv) Electron pressure p_e is constant.
v) $\overline{E} = 0$, the electric field is zero.

Let us introduce a coordinate system (x, y, z) with x-axis vertically upwards, y-axis normal to the plate directed into the fluid region, and z-axis along the width of the plate. Let $\mathbf{v} = u\widehat{i} + v\widehat{j} + w\widehat{k}$ be the velocity, $\mathbf{J} = J_x\widehat{i} + J_y\widehat{j} + J_z\widehat{k}$ be the current density at the point $p(x, y, z, t)$, and $\overline{B} = \overline{B}_0\widehat{J}$ be the applied magnetic field, $\widehat{i}$, $\widehat{j}$, $\widehat{k}$ being unit vectors along x-axis, y-axis, and z-axis respectively. Since the plate is of infinite length in x and z direction, therefore all the quantities except possibly the pressure are independent of x and z.

Now, the Eq. (2.1) gives

$$\frac{\partial \overline{v}}{\partial y} = 0, \tag{2.8}$$

which is trivially satisfied by

$$\overline{v} = -V_0, \tag{2.9}$$

where V_0 is a constant and $V_0 > 0$.

Therefore the velocity vector $\overline{v}$ is given by

$$\overline{v} = u\widehat{i} - V_0\widehat{j} + w\widehat{k}. \tag{2.10}$$

Again Eq. (2.7) is satisfied by

$$\overline{B} = \overline{B}_0\widehat{j}. \tag{2.11}$$

Also Eq. (2.5) reduces to

$$\frac{\partial J_y}{\partial y} = 0, \tag{2.12}$$

which shows that J_y = constant. Since the plate is non-conducting, $J_y = 0$ at the plate and hence $J_y = 0$ at all points in the fluid.

Thus the current density is given by

$$\overline{J} = J_x \widehat{i} + J_z \widehat{k}. \tag{2.13}$$

Under the assumption (iv) and (v), Eq. (2.6) takes the form

$$\overline{J} + \frac{m}{B_0}\left(\overline{J} \times \overline{B}\right) = \sigma\left(\overline{v} \times \overline{B}\right), \tag{2.14}$$

where $m = \omega_e \tau_e$ is the Hall parameter. Equations (2.10), (2.11), (2.13), and (2.14) yield,

$$\begin{cases} J_x = \dfrac{\sigma B_0}{1+m^2}(mu - w), \\ \\ J_z = \dfrac{\sigma B_0}{1+m^2}(u + mw). \end{cases} \tag{2.15}$$

With the following assumptions and the usual boundary layer and Boussinesq's approximation, Eqs. (2.2), (2.3), and (2.4) reduce to the following (Sharma and Chaudhary [6]):

$$\frac{\partial u}{\partial t} + v\frac{\partial u}{\partial y} = \upsilon\frac{\partial^2 u}{\partial y^2} - \frac{\sigma B_0^2(u+mw)}{\rho(1+m^2)} + g\beta(T-T_\infty) + g\beta^*(C-C_\infty) - \frac{\upsilon u}{k}, \tag{2.16}$$

$$\frac{\partial w}{\partial t} + v\frac{\partial w}{\partial y} = \upsilon\frac{\partial^2 w}{\partial y^2} + \frac{\sigma B_0^2(mu-w)}{\rho(1+m^2)} - \frac{\upsilon w}{k}, \tag{2.17}$$

$$\frac{\partial(T-T_\infty)}{\partial t} + v\frac{\partial(T-T_\infty)}{\partial y} = \frac{k}{\rho C_p}\frac{\partial^2(T-T_\infty)}{\partial y^2}, \tag{2.18}$$

$$\frac{\partial(C-C_\infty)}{\partial t} + v\frac{\partial(C-C_\infty)}{\partial y} = D\frac{\partial^2(C-C_\infty)}{\partial y^2} - K_r'(C-C_\infty). \tag{2.19}$$

In Eq. (2.18) the viscous dissipation and ohmic dissipation are ignored.

Now using $v = -V_0$, $T(y,t) - T_\infty = \theta(y,t)$ and $C(y,t) - C_\infty = C^*(y,t)$.
Subject to the boundary conditions

$$\left\{\begin{array}{l} t\leq 0 : \begin{cases} u(y,\,t) = 0, \\ w(y,\,t) = 0, \\ \theta(y,\,t) = 0, \\ C^*(y,\,t) = 0, \end{cases} \qquad \text{for all } y, \\ \\ t>0 : \begin{cases} u(y,\,t)=0,\ w(y,\,t)=0,\ \theta(y,\,t)=ae^{i\Omega t},\ C^*(y,\,t)=be^{i\Omega t} \text{ at } y=0, \\ u(y,\,t)=0,\ w(y,\,t)=0,\ \theta(y,\,t)=0,\ C^*(y,\,t)=0 \text{ as } y\to\infty. \end{cases} \end{array}\right. \tag{2.20}$$

For the sake of normalisation of the flow model and to facilitate numerical solutions, the author has to make the governing equations from (2.16) to (2.19) under the boundary conditions (2.20) dimensionless by introducing the following dimensionless quantities:

$$\begin{cases} \eta = \dfrac{V_0 y}{\upsilon},\ t' = \dfrac{V_0^2 t}{4\upsilon},\ u' = \dfrac{u}{V_0},\ w' = \dfrac{w}{V_0},\ \theta' = \dfrac{\theta}{a}, \\ C' = \dfrac{C^*}{b},\ \mathrm{Gr} = \dfrac{4g\beta\upsilon a}{V_0^3},\ K_r = \dfrac{K_r'\upsilon}{V_0^2},\ \mathrm{Gr}_c = \dfrac{4g\beta^*\upsilon b}{V_0^3},\ \mathrm{Ha} = \dfrac{4B_0^2\sigma\upsilon}{\rho V_0^3}, \\ \mathrm{Pr} = \dfrac{\upsilon\rho C_p}{\kappa},\ \mathrm{Sc} = \dfrac{\upsilon}{D},\ K = \dfrac{V_0^2 k}{4\upsilon^2},\ \omega = \dfrac{4\upsilon\Omega}{V_0^2}. \end{cases} \tag{2.21}$$

All the physical variables are defined in the nomenclature. Equations (2.16), (2.17), (2.18), and (2.19) transform to the following non-dimensional forms, respectively (dropping the dashes):

$$\frac{\partial u}{\partial t} - 4\frac{\partial u}{\partial \eta} = 4\frac{\partial^2 u}{\partial \eta^2} - \frac{\mathrm{Ha}}{(1+m^2)}(u+mw) + \mathrm{Gr}\theta + \mathrm{Gr}_c C - \frac{u}{K}, \tag{2.22}$$

$$\frac{\partial w}{\partial t} - 4\frac{\partial w}{\partial \eta} = 4\frac{\partial^2 w}{\partial \eta^2} - \frac{\mathrm{Ha}}{(1+m^2)}(w-mu) - \frac{w}{K}, \tag{2.23}$$

$$\frac{\partial \theta}{\partial t} - 4\frac{\partial \theta}{\partial \eta} = \frac{4}{\mathrm{Pr}}\frac{\partial^2 \theta}{\partial \eta^2}, \tag{2.24}$$

$$\frac{\partial C}{\partial t} - 4\frac{\partial C}{\partial \eta} = \frac{4}{\mathrm{Sc}}\frac{\partial^2 C}{\partial \eta^2} - K_r C. \tag{2.25}$$

The corresponding boundary conditions (2.20) in non-dimensional forms are as follows:

$$\begin{cases} t \le 0: & u = 0,\ w = 0,\ \theta = 0,\ C = 0 \text{ for all } \eta, \\ t > 0: & \begin{cases} u = 0,\ w = 0,\ \theta = e^{i\omega t},\ C = e^{i\omega t} \text{ at } \eta = 0, \\ u = 0,\ w = 0,\ \theta = 0,\ C = 0 \text{ as } \eta \to \infty. \end{cases} \end{cases} \tag{2.26}$$

The skin-friction, Nusselt number, and Sherwood number are important physical parameters for this type of boundary layer flow. The skin-friction at the plate, which in the non-dimensional form, is given by

$$\tau_1 = \frac{\left(\dfrac{\partial u}{\partial y}\right)_{y=0}}{\rho V_o \upsilon} = \left(\frac{\partial u}{\partial \eta}\right)_{\eta=0} \quad \text{and} \quad \tau_2 = \frac{\left(\dfrac{\partial w}{\partial y}\right)_{y=0}}{\rho V_o \upsilon} = \left(\frac{\partial w}{\partial \eta}\right)_{\eta=0}, \tag{2.27}$$

where τ_1 and τ_2 are Skin-friction coefficients along wall x-axis and z-axis respectively.

The rate of heat transfer coefficient, which is the non-dimensional form in terms of the Nusselt number (Nu) is given by

$$\mathrm{Nu} = -\frac{x}{a}\left(\frac{\partial T}{\partial y}\right)_{y=0} \quad \Rightarrow \mathrm{Nu}\,\mathrm{Re}_x^{-1} = -\left(\frac{\partial \theta}{\partial \eta}\right)_{\eta=0}. \tag{2.28}$$

The rate of mass transfer coefficient, which is the non-dimensional form in terms of the Sherwood number (Sh), is given by

$$\mathrm{Sh} = -\frac{x}{b}\left(\frac{\partial C'}{\partial y}\right)_{y=0} \quad \Rightarrow \mathrm{Sh}\,\mathrm{Re}_x^{-1} = -\left(\frac{\partial C}{\partial \eta}\right)_{\eta=0}, \tag{2.29}$$

where $\mathrm{Re} = \dfrac{V_o x}{\upsilon}$ is the local Reynolds number.

3. Method of solution

3.1. By applying Galerkin finite element method (Raju *et al.* [9]) for Eq. (2.22) over the element (e), $(\eta_j \le \eta \le \eta_k)$ is:

$$\int_{\eta_j}^{\eta_k} \left\{ N^T \left[4\frac{\partial^2 u^{(e)}}{\partial \eta^2} - \frac{\partial u^{(e)}}{\partial t} + 4\frac{\partial u^{(e)}}{\partial \eta} - Au^{(e)} + P \right] \right\} d\eta = 0, \tag{3.1}$$

where $B = \dfrac{\mathrm{Ha}}{1+m^2}$, $A = B + \dfrac{1}{K}$, $P = (\mathrm{Gr})\theta + (\mathrm{Gr}_c)C - Bmw$.

Integrating the first term in Eq. (3.1) by parts one obtains

$$
\text{(3.2)}\quad N^{(e)^T}\left\{4\frac{\partial u^{(e)}}{\partial\eta}\right\}_{\eta_j}^{\eta_k} - \int_{\eta_j}^{\eta_k}\left\{4\frac{\partial N^{(e)^T}}{\partial\eta}\frac{\partial u^{(e)}}{\partial\eta} + N^{(e)^T}\left(\frac{\partial u^{(e)}}{\partial t} - 4\frac{\partial u^{(e)}}{\partial\eta} + Au^{(e)} - P\right)\right\}d\eta = 0.
$$

Neglecting the first term in Eq. (3.2), one gets:

$$
\int_{\eta_j}^{\eta_k}\left\{4\frac{\partial N^{(e)^T}}{\partial\eta}\frac{\partial u^{(e)}}{\partial\eta} + N^{(e)^T}\left(\frac{\partial u^{(e)}}{\partial t} - 4\frac{\partial u^{(e)}}{\partial\eta} + Au^{(e)} - P\right)\right\}d\eta = 0.
$$

Let $u^{(e)} = N^{(e)}\phi^{(e)}$ be the linear piecewise approximation solution over the element $(e)\,(\eta_j \le \eta \le \eta_k)$, where $N^{(e)} = [N_j\ \ N_k]$, $\phi^{(e)} = [u_j\ \ u_k]^T$ and $N_j = \dfrac{\eta_k - \eta}{\eta_k - \eta_j}$, $N_k = \dfrac{\eta - \eta_j}{\eta_k - \eta_j}$ are the basis functions. One obtains:

$$
\int_{\eta_j}^{\eta_k}\left\{4\begin{bmatrix} N_j' N_j' & N_j' N_k' \\ N_j' N_k' & N_k' N_k' \end{bmatrix}\begin{bmatrix} u_j \\ u_k \end{bmatrix}\right\}d\eta + \int_{\eta_j}^{\eta_k}\left\{\begin{bmatrix} N_j N_j & N_j N_k \\ N_j N_k & N_k N_k \end{bmatrix}\begin{bmatrix} \dot{u}_j \\ \dot{u}_k \end{bmatrix}\right\}d\eta
$$
$$
- 4\int_{\eta_j}^{\eta_k}\left\{\begin{bmatrix} N_j N_j' & N_j N_k' \\ N_j' N_k & N_k' N_k \end{bmatrix}\begin{bmatrix} u_j \\ u_k \end{bmatrix}\right\}d\eta
$$
$$
+ A\int_{\eta_j}^{\eta_k}\left\{\begin{bmatrix} N_j N_j & N_j N_k \\ N_j N_k & N_k N_k \end{bmatrix}\begin{bmatrix} u_j \\ u_k \end{bmatrix}\right\}d\eta = P\int_{\eta_j}^{\eta_k}\begin{bmatrix} N_j \\ N_k \end{bmatrix}d\eta.
$$

Simplifying

$$
\frac{4}{l^{(e)2}}\begin{bmatrix} 1 & -1 \\ -1 & 1 \end{bmatrix}\begin{bmatrix} u_j \\ u_k \end{bmatrix} + \frac{1}{6}\begin{bmatrix} 2 & 1 \\ 1 & 2 \end{bmatrix}\begin{bmatrix} \dot{u}_j \\ \dot{u}_k \end{bmatrix}
$$
$$
- \frac{4}{2l^{(e)}}\begin{bmatrix} -1 & 1 \\ -1 & 1 \end{bmatrix}\begin{bmatrix} u_j \\ u_k \end{bmatrix} + \frac{A}{6}\begin{bmatrix} 2 & 1 \\ 1 & 2 \end{bmatrix}\begin{bmatrix} u_j \\ u_k \end{bmatrix} = \frac{P}{2}\begin{bmatrix} 1 \\ 1 \end{bmatrix},
$$

where prime and dot denotes differentiation w.r.t. η and time t respectively. Assembling the element equations for two consecutive elements $\eta_{i-1} \le \eta \le \eta_i$ and $\eta_i \le \eta \le \eta_{i+1}$ the following is obtained:

$$\frac{4}{l^{(e)^2}}\begin{bmatrix}1 & -1 & 0\\ -1 & 2 & -1\\ 0 & -1 & 1\end{bmatrix}\begin{bmatrix}u_{i-1}\\ u_i\\ u_{i+1}\end{bmatrix}+\frac{1}{6}\begin{bmatrix}2 & 1 & 0\\ 1 & 4 & 1\\ 0 & 1 & 2\end{bmatrix}\begin{bmatrix}\dot{u}_{i-1}\\ \dot{u}_i\\ \dot{u}_{i+1}\end{bmatrix}$$
$$-\frac{4}{2l^{(e)}}\begin{bmatrix}-1 & 1 & 0\\ -1 & 0 & 1\\ 0 & -1 & 1\end{bmatrix}\begin{bmatrix}u_{i-1}\\ u_i\\ u_{i+1}\end{bmatrix}+\frac{A}{6}\begin{bmatrix}2 & 1 & 0\\ 1 & 4 & 1\\ 0 & 1 & 2\end{bmatrix}\begin{bmatrix}u_{i-1}\\ u_i\\ u_{i+1}\end{bmatrix}=\frac{P}{2}\begin{bmatrix}1\\ 2\\ 1\end{bmatrix}. \tag{3.3}$$

Now put the row corresponding to the node i to zero, from Eq. (3.3) the difference in schemes with $l^{(e)}=h$ is:

$$\frac{4}{h^2}\left[-u_{i-1}+2u_i-u_{i+1}\right]+\frac{1}{6}\left[\dot{u}_{i-1}+4\dot{u}_i+\dot{u}_{i+1}\right]$$
$$-\frac{4}{2h}\left[-u_{i-1}+u_{i+1}\right]+\frac{A}{6}\left[u_{i-1}+4u_i+u_{i+1}\right]=P. \tag{3.4}$$

When applying the trapezoidal rule (3.4), the following system of equations in Crank-Nicholson method is obtained:

$$A_1u_{i-1}^{n+1}+A_2u_i^{n+1}+A_3u_{i+1}^{n+1}=A_4u_{i-1}^{n}+A_5u_i^{n}+A_6u_{i+1}^{n}+P^*, \tag{3.5}$$

where $A_1=2-12rh-Ak-24r$, $A_2=8+4Ak+48r$, $A_3=2+12rh+Ak-24r$, $A_4=2-12rh-Ak+24r$, $A_5=8-4Ak-48r$, $A_6=2+12rh+Ak+24r$, $P^*=12Pk=12k(\mathrm{Gr})\theta_i^j+12k(\mathrm{Gr}_c)C_i^j-12Bmw_i^j$.

3.2. By applying Galerkin finite element method (Raju *et al.* [9]) for Eq. (2.23) over the element (e), $(\eta_j\le\eta\le\eta_k)$ is:

$$\int_{\eta_j}^{\eta_k}\left\{N^T\left[4\frac{\partial^2 w^{(e)}}{\partial\eta^2}-\frac{\partial w^{(e)}}{\partial t}+4\frac{\partial w^{(e)}}{\partial\eta}-Aw^{(e)}+Q\right]\right\}d\eta=0, \tag{3.6}$$

where $B=\dfrac{\mathrm{Ha}}{1+m^2}$, $A=B+\dfrac{1}{K}$, $Q=Bmu$.

Integrating the first term in Eq. (3.6) by parts one obtains

$$N^{(e)^T}\left\{4\frac{\partial w^{(e)}}{\partial\eta}\right\}_{\eta_j}^{\eta_k}$$
$$-\int_{\eta_j}^{\eta_k}\left\{4\frac{\partial N^{(e)^T}}{\partial\eta}\frac{\partial w^{(e)}}{\partial\eta}+N^{(e)^T}\left(\frac{\partial w^{(e)}}{\partial t}-4\frac{\partial u^{(e)}}{\partial\eta}+Aw^{(e)}-Q\right)\right\}d\eta=0. \tag{3.7}$$

Neglecting the first term in Eq. (3.7), one gets:

$$\int_{\eta_j}^{\eta_k}\left\{4\frac{\partial N^{(e)^T}}{\partial\eta}\frac{\partial w^{(e)}}{\partial\eta}+N^{(e)^T}\left(\frac{\partial w^{(e)}}{\partial t}-4\frac{\partial w^{(e)}}{\partial\eta}+Aw^{(e)}-Q\right)\right\}d\eta=0.$$

Let $w^{(e)}=N^{(e)}\phi^{(e)}$ be the linear piecewise approximation solution over the element $(e)\,(\eta_j\le\eta\le\eta_k)$, where $N^{(e)}=[N_j\;\;N_k]$, $\phi^{(e)}=[w_j\;\;w_k]^T$ and $N_j=\dfrac{\eta_k-\eta}{\eta_k-\eta_j}$, $N_k=\dfrac{\eta-\eta_j}{\eta_k-\eta_j}$ are the basis functions. One obtains:

$$\int_{\eta_j}^{\eta_k}\left\{4\begin{bmatrix}N_j'N_j' & N_j'N_k'\\ N_j'N_k' & N_k'N_k'\end{bmatrix}\begin{bmatrix}w_j\\ w_k\end{bmatrix}\right\}d\eta+\int_{\eta_j}^{\eta_k}\left\{\begin{bmatrix}N_jN_j & N_jN_k\\ N_jN_k & N_kN_k\end{bmatrix}\begin{bmatrix}\dot{w}_j\\ \dot{w}_k\end{bmatrix}\right\}d\eta$$
$$-4\int_{\eta_j}^{\eta_k}\left\{\begin{bmatrix}N_jN_j' & N_jN_k'\\ N_j'N_k & N_k'N_k\end{bmatrix}\begin{bmatrix}w_j\\ w_k\end{bmatrix}\right\}d\eta$$
$$+A\int_{\eta_j}^{\eta_k}\left\{\begin{bmatrix}N_jN_j & N_jN_k\\ N_jN_k & N_kN_k\end{bmatrix}\begin{bmatrix}w_j\\ w_k\end{bmatrix}\right\}d\eta=Q\int_{\eta_j}^{\eta_k}\begin{bmatrix}N_j\\ N_k\end{bmatrix}d\eta.$$

Simplifying

$$\frac{4}{l^{(e)2}}\begin{bmatrix}1 & -1\\ -1 & 1\end{bmatrix}\begin{bmatrix}w_j\\ w_k\end{bmatrix}+\frac{1}{6}\begin{bmatrix}2 & 1\\ 1 & 2\end{bmatrix}\begin{bmatrix}\dot{w}_j\\ \dot{w}_k\end{bmatrix}$$
$$-\frac{4}{2l^{(e)}}\begin{bmatrix}-1 & 1\\ -1 & 1\end{bmatrix}\begin{bmatrix}w_j\\ w_k\end{bmatrix}+\frac{A}{6}\begin{bmatrix}2 & 1\\ 1 & 2\end{bmatrix}\begin{bmatrix}w_j\\ w_k\end{bmatrix}=\frac{Q}{2}\begin{bmatrix}1\\ 1\end{bmatrix},$$

where prime and dot denotes differentiation w.r.t. η and time t respectively. Assembling the element equations for two consecutive elements $\eta_{i-1}\le\eta\le\eta_i$ and $\eta_i\le\eta\le\eta_{i+1}$ the following is obtained:

$$(3.8)\quad \frac{4}{l^{(e)2}}\begin{bmatrix}1 & -1 & 0\\ -1 & 2 & -1\\ 0 & -1 & 1\end{bmatrix}\begin{bmatrix}w_{i-1}\\ w_i\\ w_{i+1}\end{bmatrix}+\frac{1}{6}\begin{bmatrix}2 & 1 & 0\\ 1 & 4 & 1\\ 0 & 1 & 2\end{bmatrix}\begin{bmatrix}\dot{w}_{i-1}\\ \dot{w}_i\\ \dot{w}_{i+1}\end{bmatrix}$$
$$-\frac{4}{2l^{(e)}}\begin{bmatrix}-1 & 1 & 0\\ -1 & 0 & 1\\ 0 & -1 & 1\end{bmatrix}\begin{bmatrix}w_{i-1}\\ w_i\\ w_{i+1}\end{bmatrix}+\frac{A}{6}\begin{bmatrix}2 & 1 & 0\\ 1 & 4 & 1\\ 0 & 1 & 2\end{bmatrix}\begin{bmatrix}w_{i-1}\\ w_i\\ w_{i+1}\end{bmatrix}=\frac{Q}{2}\begin{bmatrix}1\\ 2\\ 1\end{bmatrix}.$$

Now put the row corresponding to the node i to zero, from Eq. (3.8) the difference in schemes with $l^{(e)} = h$ is:

$$\frac{4}{h^2}\left[-w_{i-1} + 2w_i - w_{i+1}\right] + \frac{1}{6}\left[\dot{w}_{i-1} + 4\dot{w}_i + \dot{w}_{i+1}\right] - \frac{4}{2h}\left[-w_{i-1} + w_{i+1}\right] + \frac{A}{6}\left[w_{i-1} + 4w_i + w_{i+1}\right] = Q. \tag{3.9}$$

When applying the trapezoidal rule to (3.9), the following system of equations in Crank-Nicholson method is obtained:

$$B_1 w_{i-1}^{n+1} + B_2 w_i^{n+1} + B_3 w_{i+1}^{n+1} = B_4 w_{i-1}^{n} + B_5 w_i^{n} + B_6 w_{i+1}^{n} + Q^*, \tag{3.10}$$

where $B_1 = 2 - 12rh - Ak - 24r$, $B_2 = 8 + 4Ak + 48r$, $B_3 = 2 + 12rh + Ak - 24r$, $B_4 = 2 - 12rh - Ak + 24r$, $B_5 = 8 - 4Ak - 48r$, $B_6 = 2 + 12rh + Ak + 24r$, $Q^* = 12kQ = 12kAmw_i^j$.

3.3. By applying Galerkin finite element method (Raju *et al.* [9]) for Eq. (2.24) over the element (e), $(\eta_j \le \eta \le \eta_k)$ is:

$$\int_{\eta_j}^{\eta_k} \left\{ N^T \left[4\frac{\partial^2 \theta^{(e)}}{\partial \eta^2} - \Pr \frac{\partial \theta^{(e)}}{\partial t} + 4\Pr \frac{\partial \theta^{(e)}}{\partial \eta} \right] \right\} d\eta = 0. \tag{3.11}$$

Integrating the first term in Eq. (3.11) by parts one obtains

$$N^{(e)^T} \left\{ 4\frac{\partial \theta^{(e)}}{\partial \eta} \right\}_{\eta_j}^{\eta_k} - \int_{\eta_j}^{\eta_k} \left\{ 4\frac{\partial N^{(e)^T}}{\partial \eta}\frac{\partial \theta^{(e)}}{\partial \eta} + N^{(e)^T}\left(\Pr \frac{\partial \theta^{(e)}}{\partial t} - 4\Pr \frac{\partial \theta^{(e)}}{\partial \eta} \right) \right\} d\eta = 0. \tag{3.12}$$

Neglecting the first term in Eq. (3.12), one gets:

$$\int_{\eta_j}^{\eta_k} \left\{ 4\frac{\partial N^{(e)^T}}{\partial \eta}\frac{\partial \theta^{(e)}}{\partial \eta} + N^{(e)^T}\left(\Pr \frac{\partial \theta^{(e)}}{\partial t} - 4\Pr \frac{\partial \theta^{(e)}}{\partial \eta} \right) \right\} d\eta = 0.$$

Let $\theta^{(e)} = N^{(e)}\phi^{(e)}$ be the linear piecewise approximation solution over the element $(e)\,(\eta_j \le \eta \le \eta_k)$, where $N^{(e)} = [N_j \;\; N_k]$, $\phi^{(e)} = [\theta_j \;\; \theta_k]^T$ and $N_j = \dfrac{\eta_k - \eta}{\eta_k - \eta_j}$, $N_k = \dfrac{\eta - \eta_j}{\eta_k - \eta_j}$ are the basis functions. One obtains:

$$\int_{\eta_j}^{\eta_k}\left\{4\begin{bmatrix} N_j' N_j' & N_j' N_k' \\ N_j' N_k' & N_k' N_k' \end{bmatrix}\begin{bmatrix}\theta_j\\ \theta_k\end{bmatrix}\right\}d\eta + \Pr\int_{\eta_j}^{\eta_k}\left\{\begin{bmatrix} N_j N_j & N_j N_k \\ N_j N_k & N_k N_k \end{bmatrix}\begin{bmatrix}\dot\theta_j\\ \dot\theta_k\end{bmatrix}\right\}d\eta$$
$$- 4\Pr\int_{\eta_j}^{\eta_k}\left\{\begin{bmatrix} N_j N_j' & N_j N_k' \\ N_j' N_k & N_k' N_k \end{bmatrix}\begin{bmatrix}\theta_j\\ \theta_k\end{bmatrix}\right\}d\eta = 0.$$

Simplifying

$$\frac{4}{l^{(e)2}}\begin{bmatrix} 1 & -1 \\ -1 & 1 \end{bmatrix}\begin{bmatrix}\theta_j\\ \theta_k\end{bmatrix} + \frac{\Pr}{6}\begin{bmatrix} 2 & 1 \\ 1 & 2 \end{bmatrix}\begin{bmatrix}\dot\theta_j\\ \dot\theta_k\end{bmatrix} - \frac{4\Pr}{2l^{(e)}}\begin{bmatrix} -1 & 1 \\ -1 & 1 \end{bmatrix}\begin{bmatrix}\theta_j\\ \theta_k\end{bmatrix} = 0,$$

where prime and dot denotes differentiation w.r.t. η and time t respectively. Assembling the element equations for two consecutive elements $\eta_{i-1} \le \eta \le \eta_i$ and $\eta_i \le \eta \le \eta_{i+1}$ the following is obtained:

$$\frac{4}{l^{(e)2}}\begin{bmatrix} 1 & -1 & 0 \\ -1 & 2 & -1 \\ 0 & -1 & 1 \end{bmatrix}\begin{bmatrix}\theta_{i-1}\\ \theta_i \\ \theta_{i+1}\end{bmatrix} + \frac{\Pr}{6}\begin{bmatrix} 2 & 1 & 0 \\ 1 & 4 & 1 \\ 0 & 1 & 2 \end{bmatrix}\begin{bmatrix}\dot\theta_{i-1}\\ \dot\theta_i \\ \dot\theta_{i+1}\end{bmatrix}$$
$$- \frac{4\Pr}{2l^{(e)}}\begin{bmatrix} -1 & 1 & 0 \\ -1 & 0 & 1 \\ 0 & -1 & 1 \end{bmatrix}\begin{bmatrix}\theta_{i-1}\\ \theta_i \\ \theta_{i+1}\end{bmatrix} = \begin{bmatrix}0\\0\\0\end{bmatrix}. \tag{3.13}$$

Now put the row corresponding to the node i to zero, from Eq. (3.13) the difference in schemes with $l^{(e)} = h$ is:

$$\frac{4}{h^2}\left[-\theta_{i-1} + 2\theta_i - \theta_{i+1}\right] + \frac{\Pr}{6}\left[\dot\theta_{i-1} + 4\dot\theta_i + \dot\theta_{i+1}\right]$$
$$- \frac{4\Pr}{2h}\left[-\theta_{i-1} + \theta_{i+1}\right] = 0. \tag{3.14}$$

By applying the trapezoidal rule to (3.14), the following system of equations in Crank-Nicholson method is obtained:

$$C_1\theta_{i-1}^{n+1} + C_2\theta_i^{n+1} + C_3\theta_{i+1}^{n+1} = C_4\theta_{i-1}^{n} + C_5\theta_i^{n} + C_6\theta_{i+1}^{n}, \tag{3.15}$$

where $C_1 = 2(\Pr) - 12rh(\Pr) - 24r$, $C_2 = 8(\Pr) + 48r$, $C_3 = 2(\Pr) + 12rh(\Pr) - 24r$, $C_4 = 2(\Pr) - 12rh(\Pr) + 24r$, $C_5 = 8(\Pr) - 48r$, $C_6 = 2(\Pr) + 12rh(\Pr) + 24r$.

3.4. By applying Galerkin finite element method (Raju *et al.* [9]) for Eq. (2.25) over the element (e), $(\eta_j \le \eta \le \eta_k)$ is:

$$\int_{\eta_j}^{\eta_k} \left\{ N^T \left[4\frac{\partial^2 C^{(e)}}{\partial \eta^2} - \mathrm{Sc}\frac{\partial C^{(e)}}{\partial t} + 4\mathrm{Sc}\frac{\partial C^{(e)}}{\partial \eta} - (K_r)(\mathrm{Sc})\, C^{(e)} \right] \right\} d\eta = 0. \tag{3.16}$$

Integrating the first term in Eq. (3.16) by parts one obtains:

$$N^{(e)^T} \left\{ 4\frac{\partial C^{(e)}}{\partial \eta} \right\}_{\eta_j}^{\eta_k} - \int_{\eta_j}^{\eta_k} \left\{ 4\frac{\partial N^{(e)^T}}{\partial \eta}\frac{\partial C^{(e)}}{\partial \eta} + N^{(e)^T} \left(\mathrm{Sc}\frac{\partial C^{(e)}}{\partial t} - 4\mathrm{Sc}\frac{\partial C^{(e)}}{\partial \eta} + (K_r)(\mathrm{Sc})C^{(e)} \right) \right\} d\eta = 0. \tag{3.17}$$

Neglecting the first term in Eq. (3.17), one gets:

$$\int_{\eta_j}^{\eta_k} \left\{ 4\frac{\partial N^{(e)^T}}{\partial \eta}\frac{\partial C^{(e)}}{\partial \eta} + N^{(e)^T} \left(\mathrm{Sc}\frac{\partial C^{(e)}}{\partial t} - 4\mathrm{Sc}\frac{\partial C^{(e)}}{\partial \eta} + (K_r)(\mathrm{Sc})C^{(e)} \right) \right\} d\eta = 0.$$

Let $C^{(e)} = N^{(e)}\phi^{(e)}$ be the linear piecewise approximation solution over the element $(e)\,(\eta_j \le \eta \le \eta_k)$, where $N^{(e)} = [N_j \;\; N_k]$, $\phi^{(e)} = [C_j \;\; C_k]^T$ and $N_j = \dfrac{\eta_k - \eta}{\eta_k - \eta_j}$, $N_k = \dfrac{\eta - \eta_j}{\eta_k - \eta_j}$ are the basis functions. One obtains:

$$\begin{aligned} &\int_{\eta_j}^{\eta_k} \left\{ 4\begin{bmatrix} N_j' N_j' & N_j' N_k' \\ N_j' N_k' & N_k' N_k' \end{bmatrix} \begin{bmatrix} C_j \\ C_k \end{bmatrix} \right\} d\eta + \mathrm{Sc}\int_{\eta_j}^{\eta_k} \left\{ \begin{bmatrix} N_j N_j & N_j N_k \\ N_j N_k & N_k N_k \end{bmatrix} \begin{bmatrix} \dot{C}_j \\ \dot{C}_k \end{bmatrix} \right\} d\eta \\ &\qquad - 4\mathrm{Sc}\int_{\eta_j}^{\eta_k} \left\{ \begin{bmatrix} N_j N_j' & N_j N_k' \\ N_j' N_k & N_k' N_k \end{bmatrix} \begin{bmatrix} C_j \\ C_k \end{bmatrix} \right\} d\eta \\ &\qquad + (K_r)(\mathrm{Sc})\int_{\eta_j}^{\eta_k} \left\{ \begin{bmatrix} N_j N_j & N_j N_k \\ N_j N_k & N_k N_k \end{bmatrix} \begin{bmatrix} C_j \\ C_k \end{bmatrix} \right\} d\eta = 0. \end{aligned}$$

Simplifying

$$\frac{4}{l^{(e)2}}\begin{bmatrix} 1 & -1 \\ -1 & 1 \end{bmatrix}\begin{bmatrix} C_j \\ C_k \end{bmatrix} + \frac{\mathrm{Sc}}{6}\begin{bmatrix} 2 & 1 \\ 1 & 2 \end{bmatrix}\begin{bmatrix} \dot{C}_j \\ \dot{C}_k \end{bmatrix} - \frac{4\mathrm{Sc}}{2l^{(e)}}\begin{bmatrix} -1 & 1 \\ -1 & 1 \end{bmatrix}\begin{bmatrix} C_j \\ C_k \end{bmatrix} + \frac{(K_r)\,(\mathrm{Sc})}{6}\begin{bmatrix} 2 & 1 \\ 1 & 2 \end{bmatrix}\begin{bmatrix} C_j \\ C_k \end{bmatrix} = 0,$$

where prime and dot denotes differentiation w.r.t. η and time t respectively. Assembling the element equations for two consecutive elements $\eta_{i-1} \leq \eta \leq \eta_i$ and $\eta_i \leq \eta \leq \eta_{i+1}$ the following is obtained:

$$\frac{4}{l^{(e)2}}\begin{bmatrix} 1 & -1 & 0 \\ -1 & 2 & -1 \\ 0 & -1 & 1 \end{bmatrix}\begin{bmatrix} C_{i-1} \\ C_i \\ C_{i+1} \end{bmatrix} + \frac{\mathrm{Sc}}{6}\begin{bmatrix} 2 & 1 & 0 \\ 1 & 4 & 1 \\ 0 & 1 & 2 \end{bmatrix}\begin{bmatrix} \dot{C}_{i-1} \\ \dot{C}_i \\ \dot{C}_{i+1} \end{bmatrix} - \frac{4\mathrm{Sc}}{2l^{(e)}}\begin{bmatrix} -1 & 1 & 0 \\ -1 & 0 & 1 \\ 0 & -1 & 1 \end{bmatrix}\begin{bmatrix} C_{i-1} \\ C_i \\ C_{i+1} \end{bmatrix} + \frac{(K_r)\,(\mathrm{Sc})}{6}\begin{bmatrix} 2 & 1 & 0 \\ 1 & 4 & 1 \\ 0 & 1 & 2 \end{bmatrix}\begin{bmatrix} C_{i-1} \\ C_i \\ C_{i+1} \end{bmatrix} = \begin{bmatrix} 0 \\ 0 \\ 0 \end{bmatrix}. \tag{3.18}$$

Now put the row corresponding to the node i to zero, from Eq. (3.18) the difference in schemes with $l^{(e)} = h$ is:

$$\frac{4}{h^2}\left[-C_{i-1} + 2C_i - C_{i+1}\right] + \frac{1}{6}\left[\dot{C}_{i-1} + 4\dot{C}_i + \dot{C}_{i+1}\right] - \frac{4}{2h}\left[-C_{i-1} + C_{i+1}\right] + \frac{(K_r)(\mathrm{Sc})}{6}\left[C_{i-1} + 4C_i + C_{i+1}\right] = 0. \tag{3.19}$$

By applying the trapezoidal rule to (3.19), the following system of equations in Crank-Nicholson method is obtained:

$$D_1 C_{i-1}^{n+1} + D_2 C_i^{n+1} + D_3 C_{i+1}^{n+1} = D_4 C_{i-1}^{n} + D_5 C_i^{n} + D_6 C_{i+1}^{n}, \tag{3.20}$$

where $D_1 = 2(\mathrm{Sc}) + 12rh(\mathrm{Sc}) - (K_r)(\mathrm{Sc})k - 24r$, $D_2 = 8(\mathrm{Sc}) - 4(K_r)(\mathrm{Sc})k + 48r$, $D_3 = 2(\mathrm{Sc}) - 12rh(\mathrm{Sc}) + (K_r)(\mathrm{Sc})k - 24r$, $D_4 = 2(\mathrm{Sc}) - 12rh(\mathrm{Sc}) - (K_r)(\mathrm{Sc})k + 24r$, $D_5 = 8(\mathrm{Sc}) + 4(K_r)(\mathrm{Sc})k - 48r$, $D_6 = 2(\mathrm{Sc}) + 12rh(\mathrm{Sc}) + (K_r)(\mathrm{Sc})k + 24r$.

Here $r = \dfrac{k}{h^2}$ and h, k are mesh sizes along η-direction and time-direction respectively. Index i refers to space and j refers to the time. In Eqs. (3.5), (3.10), (3.15), and (3.20) taking $i = 1(1)n$ and using boundary conditions (2.26), the following system of equations is obtained:

$$A_i X_i = B_i, \qquad i = 1(1)n, \tag{3.21}$$

where A_i are matrices of order n and X_i, B_i are column matrices having n – components. The solutions of the above system of equations are obtained by using Thomas algorithm for velocity, temperature, and concentration. Also, numerical solutions for these equations are obtained by C-programme. In order to prove the convergence and stability of Galerkin finite element method, the same C-programme was run with smaller values of h and k and no significant change was observed in the values of u, w, θ, and C. Hence, using Galerkin finite element method, the result was stable and convergent.

4. Results and discussions

The similarity Eqs. (2.22), (2.23), (2.24), and (2.25) were solved numerically subject to the boundary conditions given by (2.26). Graphical representations of the numerical results are illustrated in Fig. 2 to Fig. 14 to show the influences of different numbers on the boundary layer flow. In this study, the influence of the effects of material parameters such as Prandtl number, Schmidt number, Hartmann number, Hall parameter, Grashof number for heat transfer, Grashof number for mass transfer, and chemical reaction have been investigated separately in order to clearly observe their respective effects on the velocity, temperature, and concentration profiles of the flow. Also the numerical results of skin-friction coefficients, rate of heat and mass transfer coefficients in terms of Nusselt number and Sherwood number respectively have been observed through graphically. During the course of numerical calculations of the primary velocity, secondary velocity, temperature and concentration, the values of the Prandtl number were chosen for mercury (Pr = 0.025), air at 25°C and one atmospheric pressure (Pr = 0.71), water (Pr = 7.00), and water at 4°C (Pr = 11.40). To focus atten-

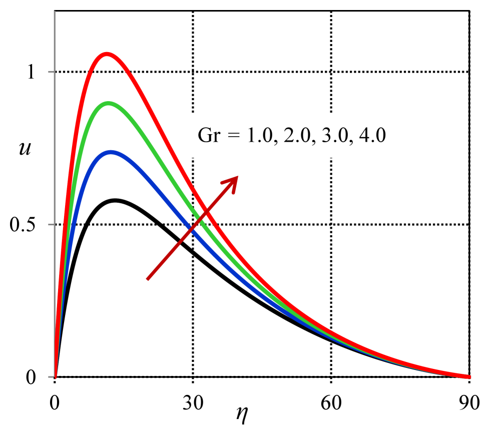

Fig. 2. Effect of Grashof number for heat transfer Gr on u.

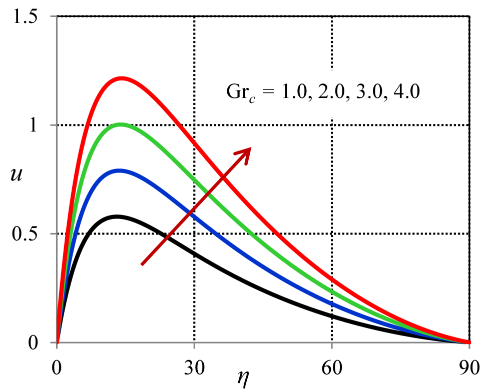

Fig. 3. Effect of Grashof number for mass transfer Gr_c on u.

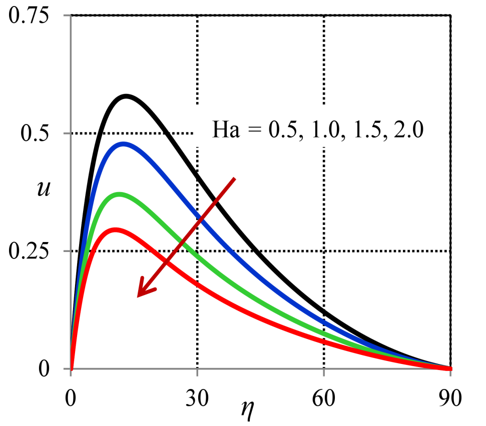

FIG. 4. Effect of Hartmann number Ha on u.

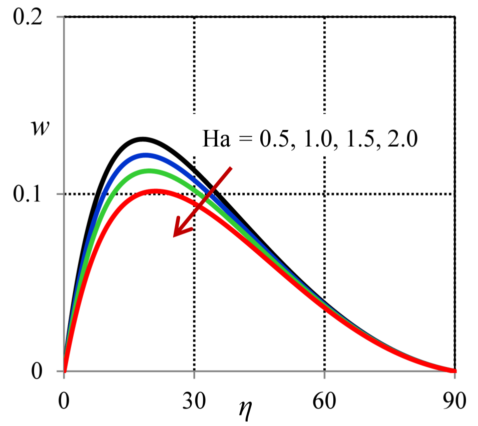

FIG. 5. Effect of Hartmann number Ha on w.

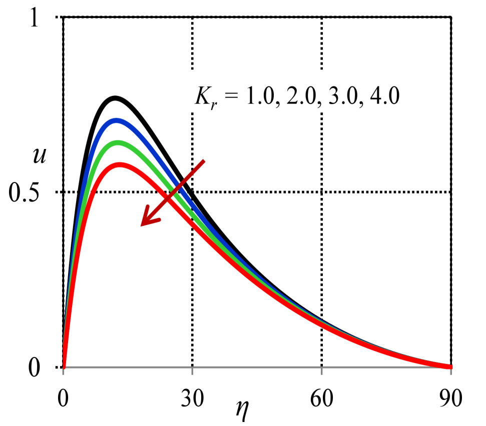

FIG. 6. Effect of the chemical reaction parameter K_r on u.

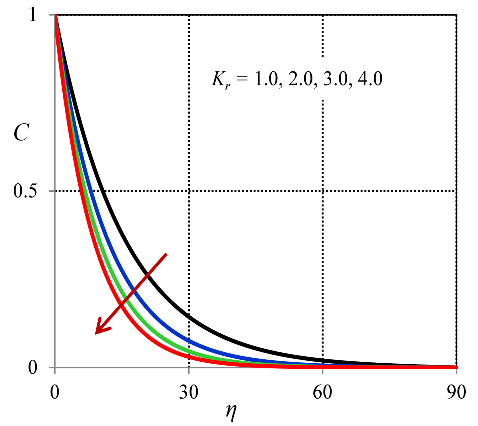

FIG. 7. Effect of the chemical reaction parameter K_r on C.

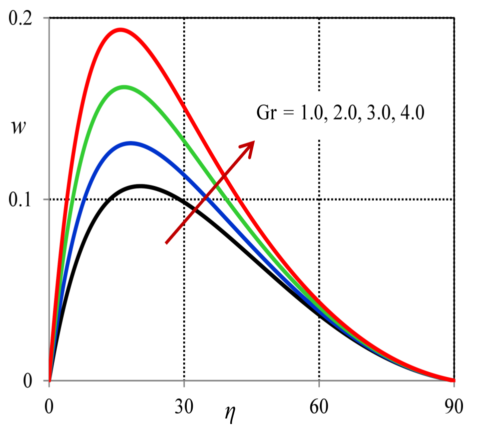

FIG. 8. Effect of Grashof number for heat transfer Gr on w.

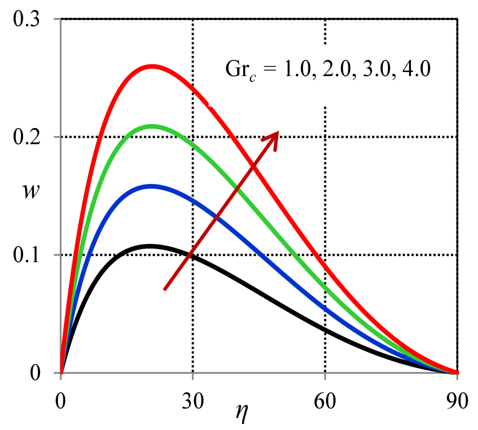

FIG. 9. Effect of Grashof number for mass transfer Gr_c.

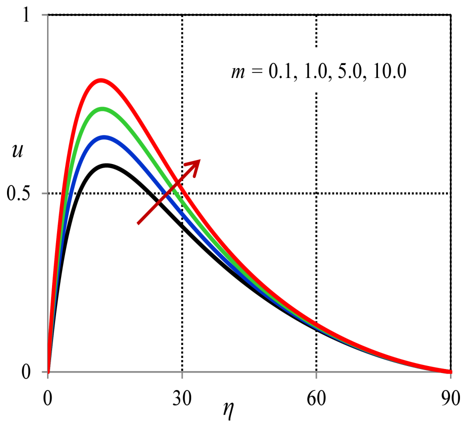

FIG. 10. Effect of Hall parameter m on u.

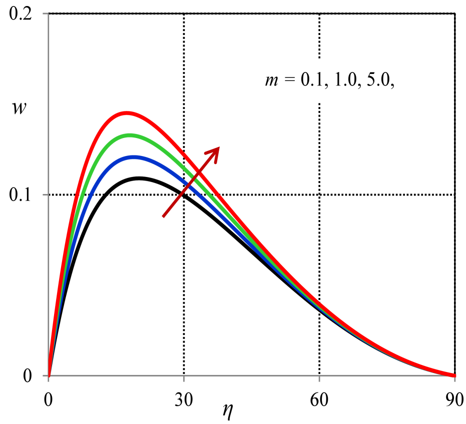

FIG. 11. Effect of Hall parameter m on w.

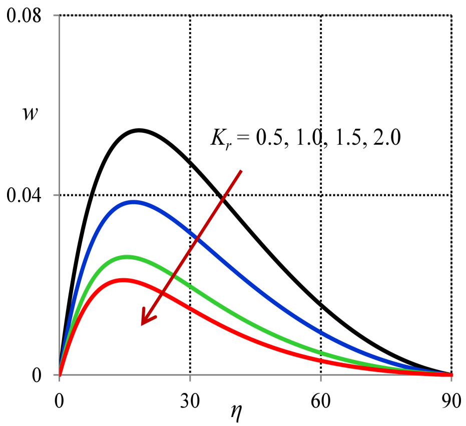

FIG. 12. Effect of the chemical reaction parameter K_r on w.

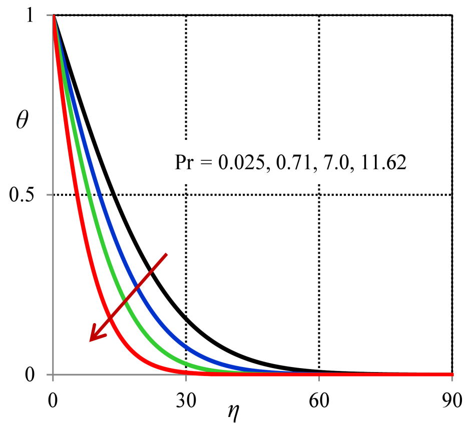

FIG. 13. Effect of Prandtl number Pr on θ.

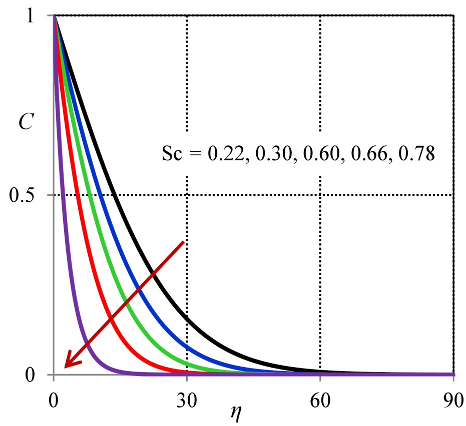

FIG. 14. Effect of Schmidt number Sc on C.

tion on numerical values of the results obtained in the study the values of Sc were chosen for the gases representing diffusing chemical species of most common interest in air, namely, hydrogen (Sc = 0.22), helium (Sc = 0.30), water vapour (Sc = 0.60), oxygen (Sc = 0.66), and ammonia (Sc = 0.78). For the physical significance, the numerical discussions in the problem and at $t = 1.0$, $\omega t = \pi/2$ stable values for velocity, temperature, and concentration fields were obtained. To find a solution of this problem, an infinite vertical plate was placed in a finite length in the flow. Hence, the entire problem in a finite boundary was solved. However, in the graphs, the η values vary from 0 to 90. The velocity, temperature, and concentration tend to zero as η tends to 90. This is true for any value of η. Thus, a finite length was considered in this study. The temperature and the species concentration are coupled to the velocity via the Grashof number, the modified Grashof number as seen in Eq. (2.22). The effects of Grashof numbers for heat and mass transfer are illustrated in Fig. 2 and Fig. 3 respectively. The Grashof number for heat transfer signifies the relative effect of the thermal buoyancy force to the viscous hydrodynamic force in the boundary layer. As expected, it is observed that there was a rise in the velocity due to the enhancement of thermal buoyancy force. Also, as Gr increases, the peak values of the velocity increases rapidly near the porous plate and then decays smoothly to the free stream velocity. The Grashof number for mass transfer defines the ratio of the species buoyancy force to the viscous hydrodynamic force. As expected, the fluid velocity increases and the peak value is more distinctive due to increase in the species buoyancy force. The velocity distribution attains a distinctive maximum value in the vicinity of the plate and then decreases properly to approach the free stream value. It is noticed that the velocity increases with increasing values of the Grashof number for mass transfer.

Figures 4 and 5 display the effect of magnetic field parameter or Hartmann number (Ha) on primary and secondary velocities. It is seen from these figures that the primary as well as secondary velocity falls when Ha increases. That is the primary or secondary fluid motion is retarded due to application of transverse magnetic field. This phenomenon clearly agrees with the fact that Lorentz force that appears due to interaction of the magnetic field and fluid velocity resists the fluid motion. Figure 6 illustrates the behaviour of primary velocity profiles for different values of the chemical reaction parameter (K_r). It is pertinent to mention that $K_r > 0$ corresponds to a destructive chemical reaction. It can be seen from the profiles that the primary velocity reduces in the degenerating chemical reaction in the boundary layer. This is due to the fact that the increase in the rate of chemical reaction rate leads to thinning of a momentum in a boundary layer in degenerating chemical reaction. It can be seen from the profiles that the cross flow primary velocity reduces in the degenerating chemical reaction. Figure 7 shows a destructive type of chemical reaction because the concentration decreases for increasing chemical reaction parameter which indicates that the diffusion rates can be tremendously changed by a chemical reaction. This is due to the fact that an increase in the chemical reaction K_r causes the concentration at the boundary layer to become thinner, which decreases the concentration of the diffusing species. This decrease in the concentration of the diffusing species diminishes the mass diffusion.

The influence of both heat and mass transfer coefficients (Grashof numbers for heat and mass transfer) on secondary velocity profiles is as shown in Figs. 8 and 9 respectively. As both the heat and mass transfer increase, this velocity component increases as well. The influence of the hall parameter m on primary and secondary velocity profiles is as shown in Figs. 10 and 11 respectively. It is observed from these figures that the primary and secondary velocity profiles increase with an increase in the hall parameter m. This is because, in general, the Hall currents reduce the resistance offered by the Lorentz force. This means that Hall currents have a tendency to increase the fluid velocity components. Figure 12 shows the effect of the chemical reaction parameter on the secondary velocity. It can be seen that as the values of this parameter increase, the secondary velocity also increases. Figure 13 depicts the temperature profiles against η taking different values of Prandtl number (Pr). It is clear from this figure that as Prandtl number increases, the temperature profile decreases. This is because the fluid is highly conductive for a small value of Prandtl number. Physically, if Prandtl number increases, the thermal diffusivity decreases, and this phenomenon leads to the decreasing manner of the energy transfer ability that reduces the thermal boundary layer. Figure 14 displays concentration profiles C vs. η for various gases like hydrogen ($\mathrm{Sc} = 0.22$), helium ($\mathrm{Sc} = 0.30$), water vapour ($\mathrm{Sc} = 0.60$), oxygen ($\mathrm{Sc} = 0.66$) and ammonia ($\mathrm{Sc} = 0.78$). It is reported that the effect of increasing values of Schmidt number (Sc) is to decrease the concentration profiles. This is consistent with the fact that the increase of Sc means a decrease of molecular diffusivity (D) which results in decrease of concentration boundary layer. Hence, the concentration of species is higher for smaller values of Sc and lower for larger values of Sc. Furthermore, it is observed that near the boundary the thickness of the concentration boundary layer increases significantly with increasing frequency but an opposite trend is noted far away from the plate ($\eta > 30$).

The profiles for skin-friction (τ_1) due to primary velocity under the effects of Grashof number for heat transfer, Grashof number for mass transfer, Schmidt number, Prandtl number, Hartmann number, Hall parameter, Permeability of porous medium, and chemical reaction are presented in Table 1. From the above Table 1, the skin-friction due to primary velocity rises under the effects of Grashof number for heat transfer, Grashof number for mass transfer, Hall parameter, Permeability of porous medium and falls under the effects of

Table 1. Skin-friction ($\tau_1 \& \tau_2$) results.

Gr	Gr_c	Sc	Pr	Ha	m	K	K_r	τ_1	τ_2
1.0	1.0	0.21	0.71	1.0	1.0	1.0	1.0	2.05142214	0.54749974
2.0	1.0	0.21	0.71	1.0	1.0	1.0	1.0	2.91523360	0.76566248
1.0	2.0	0.21	0.71	1.0	1.0	1.0	1.0	3.23890159	0.87655102
1.0	1.0	0.30	0.71	1.0	1.0	1.0	1.0	2.00551483	0.53103365
1.0	1.0	0.21	7.00	1.0	1.0	1.0	1.0	1.20460657	0.33252418
1.0	1.0	0.21	0.71	2.0	1.0	1.0	1.0	1.82362254	0.58930248
1.0	1.0	0.21	0.71	1.0	2.0	1.0	1.0	2.11262295	0.86450064
1.0	1.0	0.21	0.71	1.0	1.0	2.0	1.0	2.32723154	0.55901425
1.0	1.0	0.21	0.71	1.0	1.0	1.0	2.0	1.86543369	0.58240181

Schmidt number, Prandtl number, Hartmann number, and chemical reaction. The profiles for skin-friction (τ_2) due to secondary velocity under the effects of Grashof number for heat transfer, Grashof number for mass transfer, Schmidt number, Prandtl number, Hartmann number, Hall parameter, Permeability of Porous medium, and Chemical reaction are presented in Table 1. From the above Table 1 the skin-friction due to secondary velocity increases under the effects Grashof number for heat transfer, Grashof number for mass transfer, Hartmann number, Hall parameter, Permeability of porous medium, and chemical reaction. And the skin-friction decreases under the effects of Schmidt number and Prandtl number. From Table 2 it is seen that an increase in Prandtl number leads to decrease in Nusselt number. The Prandtl number is a measure of relative importance of heat conduction and viscosity of a flow. The careful study of Table 2 reveals that for higher values of $\mathrm{Pr} = 7.0$ (i.e., for water) the Nusselt number decreases significantly. This shows that when viscosity of a fluid dominates over conductivity then the rate of heat transfer decreases significantly. The profiles for Sherwood number due to concentration profiles under the effect of Schmidt number and chemical reaction are presented in Table 2. From Table 2 one can see that the Sherwood number due to concentration profile decreases under the effects of Schmidt number and chemical reaction.

Table 2. Rate of heat and mass transfer (Nu & Sh) values.

Pr	Nu	Sc	K_r	Sh
0.71	5.93614136	0.22	1.0	0.09151846
7.00	4.01793025	0.30	1.0	0.07492118
0.71	5.93614136	0.22	2.0	0.06648447

5. Program validation and comparison with previous research

In order to assess the accuracy of current finite element method, the author has compared the results with accepted data sets for the rate of mass transfer for a case of magnetohydrodynamic viscous incompressible fluid flow past a vertical porous plate immersed in porous medium in presence of hall current, corresponding to the case computed by Sharma and Chaudhary [6], in the absence of chemical reaction by taking different values for Schmidt number and phase angle keeping the other parameters fixed and these results are presented in Table 3. These favourable comparisons lend confidence in the accuracy of the numerical procedure. Therefore, the developed code can be used with great confidence confidence to study the problem considered in this paper.

Table 3. Sh is the rate of mass transfer (Sherwood number) results obtained in the present study, and $C(t)$ is the rate of mass transfer results obtained by Sharma and Chaudhary.

		$C(t)$ (Analytical results of Sharma and Chaudhary [6])			Sh (Present numerical results)		
$\omega\downarrow$	Sc $\rightarrow$	0.22	0.30	0.78	0.22	0.30	0.78
0.0		0.2200	0.3000	0.7800	0.2200	0.3000	0.7800
0.2		0.0800	0.1200	0.3800	0.0812	0.1274	0.3875
0.4		−0.1700	−0.2100	−0.4100	−0.1747	−0.2151	−0.4162
0.6		−0.2700	−0.3500	−0.8100	−0.2755	−0.3594	−0.8188
0.8		−0.0800	−0.1200	0.3900	−0.0832	−0.1277	0.3934
1.0		0.2100	0.2600	0.4400	0.2137	0.2638	0.4492

6. Conclusions

This work investigated the effect of chemical reaction on an unsteady magnetohydrodynamic free convection flow past a vertical porous plate immersed in a porous medium with hall current. The similar solutions were obtained using suitable transformations and the resulting similar ordinary differential equations were solved by using Galerkin finite element method (Raju *et al.* [9]). A parametric study illustrating the influence of different flow parameters on velocity, temperature, and concentration fields were investigated. The shearing stress at the plate due to primary and secondary velocity fields and rate of heat and mass transfer due to temperature and concentration respectively were obtained in a non-dimensional form. The results are presented graphically and in tables. The author concluded that the flow field and the quantities of physical interest are significantly influenced by these numbers.

1. The primary and secondary motion is retarded under the effects of transverse magnetic field due to the magnetic pull of the Lorentz force acting on the flow field, whereas this motion is accelerated under Hall effect.
2. The fluid motion is retarded due to chemical reaction. Hence, the consumption of chemical species causes a fall in the concentration field which in turn diminishes the buoyancy effects due to concentration gradients. Hence the flow field is retarded.
3. Due to the chemical reaction, the concentration of the fluid decreases. This is because the consumption of chemical species leads to a fall in the species concentration field.
4. It was found that when the Grashof numbers for heat and mass transfer were increased, the thermal and concentration buoyancy effects were enhanced and thus, the primary and secondary velocities increased.
5. The concentration profiles of the flow field decreases at all the points as the Schmidt number increases. This means the heavier diffusing species have a greater retarding effect on the concentration profiles of the flow field.
6. The Prandtl number reduces the temperature of the flow field at all points. The higher the Prandtl number, the sharper the reduction in temperature of the flow field.
7. The obtained results for special cases of the problem were compared with previously published work and found to be in good agreement.

Future research work with respect to the present one. It can be stated for future research work that for this research problem and scope finite element method is very useful method for solving linear and non-linear partial and ordinary differential equations in physics, mechanical engineering, etc. The results obtained are quite accurate as compared to other numerical methods. Mechanical engineers use this method to solve complex problems that arise in their research problems.

Applications of this research work. The present problem has significant applications in soil mechanics, water purification, powder metallurgy, study of the interaction of the geomagnetic field within the geothermal region, the petroleum engineering concerned with the movement of oil, gas, and water through the reservoirs. It is hoped that the results will be useful for applications including nuclear engineering, especially in designing more efficient cooling systems for nuclear reactors, and that they can also be used for comparison with other problems dealing with Hall current which might be more complicated. It is also hoped that the results can serve as a complement to other studies.

Acknowledgment

The author is grateful to the reviewers for their valuable comments and suggestions which helped them to improve the quality of this research paper. Also the author is thankful to Dr. K. Tejaswani, GITAM University for her suggestions, support, and encouragement in the preparation of this manuscript.

References

1. Nield D.A., Bejan A., *Convection in porous media*, 2nd Edition, Springer Verlag, Berlin, 1998.
2. Hiremath P.S., Patil P.M., *Free convection effects on oscillatory flow of couple stress field through a porous medium*, Acta Mechanica, **98**(1–4): 143–158, 1993.
3. Sharma B.K., Chaudhary R.C., Sharma P.K., *Fluctuating mass transfer on three dimensional flow through a porous medium with variable permeability*, Advances in Theoretical and Applied Mathematics, **2**(3): 257–267, 2007.
4. Helmy K.A., *MHD unsteady free convection flow past a vertical porous plate*, ZAMM, **98**(4): 255–270, 1998.
5. Chaudhary R.C., Sharma B.K., *Combined heat and mass transfer by laminar mixed convection flow from a vertical surface with induced magnetic field*, Journal of Applied Physics, **99**(3): 3401–3410, 2006, doi:10.1063/1.2161817.
6. Sharma B.K., Chaudhary R.C., *Hydromagnetic unsteady mixed convection and mass transfer flow past a vertical porous plate immersed in a porous medium with Hall Effect*, Engineering Transactions, **56**(1): 3–23, 2008.
7. El-Amin M.F., *Magnetohydrodynamic free convection and mass transfer flow in micropolar fluid with constant suction*, Journal of Magnetism and Magnetic Materials, **234**(3): 567–574, 2001, doi:10.1016/S0304–8853(01)00374–2.
8. Ramana Murthy M.V., Srinivasa Raju R., Anand Rao J., *Heat and mass transfer effects on MHD natural convective flow past an infinite vertical porous plate with thermal radiation and Hall current*, Procedia Engineering Journal, **127**: 1330–1337, 2015.
9. Raju R.S., Sudhakar K., Rangamma M., *The effects of thermal radiation and heat absorption on an unsteady MHD free convection flow past an infinite vertical plate with thermal diffusion and diffusion thermo*, Journal of Institution of Engineers (India): Series C, **94**: 175–186, 2013.
10. Anand Rao J., Srinivasa Raju R., *The effects of Hall currents, Soret and Dufour on MHD flow and heat transfer along a porous flat plate with mass transfer*, Journal of Energy, Heat and Mass Transfer, **33**: 351–372, 2011.
11. Siva Reddy Sheri, Srinivasa Raju R., *Soret effect on unsteady MHD free convective flow past a semi-infinite vertical plate in the presence viscous dissipation*, International Journal of Computational Methods in Engineering Science and Mechanics, **16**(2): 132–141, 2015.
12. Siva Reddy Sheri, Srinivasa Raju R., *Transient MHD free convective flow past an infinite vertical plate embedded in a porous medium with viscous dissipation*, Meccanica, **51**(5): 1057–1068, 2016.

13. Sivaiah S., Srinivasa Raju R., *Finite element solution of heat and mass transfer flow with Hall current Heat Absorption and viscous dissipation*, Applied Mathematics and Mechanics (English Edition), **34**: 559–570, 2013.

14. Rao V.S., Babu L.A., Raju R.S., *Finite element analysis of radiation and mass transfer flow past semi – infinite moving vertical plate with viscous dissipation*, Journal of Applied Fluid Mechanics, **6**(3): 321–329, 2013.

15. Anand Rao J., Srinivasa Raju R., Sivaiah S., *Finite element solution of MHD transient flow past an impulsively started infinite horizontal porous plate in a rotating fluid with Hall current*, Journal of Applied Fluid Mechanics, **5**(3): 105–112, 2012.

16. Anand Rao J., Srinivasa Raju R., Sivaiah S., *Finite element solution of heat and mass transfer in MHD flow of a viscous fluid past a vertical plate under oscillatory suction velocity*, Journal of Applied Fluid Mechanics, **5**(3): 1–10, 2012.

17. Cussler E.L., *Diffusion mass transfer in fluid systems*, 2nd Edition, Cambridge University Press, Cambridge, 1998.

18. Das U.N., Deka R.K., Soundalgekar V.M., *Effects of mass transfer on flow past an impulsively started infinite vertical plate with constant heat flux and chemical reaction*, Forschung im Ingenieurwesen, **60**(10): 284–287, 1994, doi:10.1007/BF02601318.

19. Muthucumarswamy R., Ganesan P., *First order chemical reaction on flow past an impulsively started vertical plate with uniform heat and mass flux*, Acta Mechanica, **147**(1–4): 45–57, 2001, doi:10.1007/BF01182351.

20. Muthucumarswamy R., *Effects of a chemical reaction on moving isothermal vertical surface with suction*, Acta Mechanica, **155**(1–2): 65–70, 2002.

21. Das U.N., Deka R., Soundalgekar V.M., *Effects of mass transfer on flow past an impulsively started infinite vertical plate with constant heat flux and chemical reaction*, Forschung im Ingenieurwesen/Engineering Research, **60(**10): 284–287, 1994.

22. Anjali Devi S.P., Kandasamy R.K., *Effects of chemical reaction, heat and mass transfer on laminar flow along a semi infinite horizontal plate*, Heat and Mass Transfer, **35**(6): 465–467, 1999.

23. Seddeek M.A., Darwish A.A., Abdelmeguid M.S., *Effects of chemical reaction and variable viscosity on hydromagnetic mixed convection heat and mass transfer for Hiemenz flow through porous media with radiation*, Communications in Nonlinear Science and Numerical Simulation, **12**(2): 195–213, 2007.

24. Patil P.M., Kulkarni P.S., *Effects of chemical reaction on free convective flow of a polar fluid through a porous medium in the presence of internal heat generation*, International Journal of Thermal Sciences, **47**(8): 1043–1054, 2008.

25. Salem A.M., Abd El-Aziz M., *Effect of Hall currents and chemical reaction on hydromagnetic flow of a stretching vertical surface with internal heat generation/absorption*, Applied Mathematical Modeling, **32**(7): 1236–1254, 2008.

26. Ibrahim F.S., Elaiw A.M., Bakr A.A., *Effect of the chemical reaction and radiation absorption on the unsteady MHD free convection flow past a semi infinite vertical permeable moving plate with heat source and suction*, Communications in Nonlinear Science and Numerical Simulation, **13**(6): 1056–1066, 2008.

27. Parida S.K., Acharya M., Dash G.C., Panda S., *MHD heat and mass transfer in a rotating system with periodic suction*, Arabian Journal for Science and Engineering, **36**(6): 1139–1151, 2011.

28. Rajeswari R., Jothiram B., Nelson V.K., *Chemical reaction, heat and mass transfer on Nonlinear MHD boundary layer flow through a vertical porous surface in the presence of suction*, Applied Mathematical Sciences, **3**(49–52): 2469–2480, 2009.

29. Mahdy A., *Effect of chemical reaction and heat generation or absorption on double diffusive convection from a vertical truncated cone in porous media with variable viscosity*, International Communications in Heat and Mass Transfer, **37**(5): 548–554, 2010.

30. Muthucumaraswamy R., Ravi Shankar M., *First order chemical reaction and thermal radiation effects on unsteady flow past an accelerated isothermal infinite vertical plate*, Indian Journal of Science and Technology, **4**(5): 573–577, 2011.

31. Jithender Reddy G., Anand Rao J., Srinivasa Raju R., *Chemical reaction and radiation effects on MHD free convection from an impulsively started infinite vertical plate with viscous dissipation*, International Journal of Advances in Applied Mathematics and Mechanics, **2**(3): 164–176, 2015.

32. Sudhakar K., Srinivasa Raju R., Rangamma M., *Hall effect on an unsteady MHD flow past along a porous flat plate with thermal diffusion, diffusion thermo and chemical reaction*, Journal of Physical and Mathematical Sciences, **4**(1): 370–395, 2013.

33. Sudhakar K., Srinivasa Raju R., Rangamma M., *Chemical reaction effect on an unsteady MHD free convection flow past an infinite vertical accelerated plate with constant heat flux, thermal diffusion and diffusion thermo*, International Journal of Modern Engineering Research, **2**(5): 3329–3339, 2012.

34. Anand Rao J., Sivaiah S., Srinivasa Raju R., *Chemical Reaction effects on an unsteady MHD free convection fluid flow past a semi-infinite vertical plate embedded in a porous medium with heat absorption*, Journal of Applied Fluid Mechanics, **5**(3): 63–70, 2012.

35. Srinivasa Raju R., *Combined influence of thermal diffusion and diffusion thermo on unsteady hydromagnetic free convective fluid flow past an infinite vertical porous plate in presence of chemical reaction*, Journal of Institution of Engineers (India), **Series C**: 1–11, 2016, doi: 10.1007/s40032-016-0258-5.

36. Srinivasa Raju R., Mahesh Reddy B., Rashidi M.M., Gorla R.S.R., *Application of finite element method to unsteady MHD free convection flow past a vertically inclined porous plate including thermal diffusion and diffusion thermo effects*, Journal of Porous Media, 2016 (in Press).

37. Srinivasa Raju R., Jithender Reddy G., Anand Rao J., Rashidi M.M., Gorla R.S.R., *Analytical and Numerical study of unsteady MHD free convection flow over an exponentially moving vertical plate with heat absorption*, International Journal of Thermal Sciences, **107**: 303–315, 2016.

Received August 30, 2014; accepted version June 25, 2016.